Differential Regulation of Opposing Rel_{Mtb} Activities by the Aminoacylation State of a tRNA·Ribosome·mRNA·Rel_{Mtb} Complex†

David Avarbock, Andrew Avarbock, and Harvey Rubin*

Division of Infectious Diseases, Department of Medicine, School of Medicine, University of Pennsylvania, Philadelphia, Pennsylvania 19104

Received June 1, 2000; Revised Manuscript Received July 20, 2000

ABSTRACT: Rel_{Mtb} of *Mycobacterium tuberculosis* is responsible for the intracellular regulation of (p)ppGpp and the consequent ability of the organism to survive long-term starvation, indicating a possible role in the pathogenesis of tuberculosis. Purified Rel_{Mtb} is a dual-function enzyme carrying out ATP:GTP/GDP/ITP 3′-pyrophosphoryltransferase and (p)ppGpp 3′-pyrophosphohydrolase reactions. Here we show that in the absence of biological regulators, Rel_{Mtb} simultaneously catalyzes both transferase and hydrolysis at the maximal rate for each reaction, indicating the existence of two distinct active sites. The differential regulation of the opposing activities of Rel_{Mtb} is dependent on the ratio of uncharged to charged tRNA and the association of Rel_{Mtb} with a complex containing tRNA, ribosomes, and mRNA. A 20-fold increase in the k_{cat} and a 4-fold decrease in K_{ATP} and K_{GTP} from basal levels for transferase activity occur when Rel_{Mtb} binds to a complex containing uncharged tRNA, ribosomes, and mRNA (Rel_{Mtb} activating complex or RAC). The k_{cat} for hydrolysis, however, is reduced 2-fold and K_m for pppGpp increased 2-fold from basal levels in the presence of the Rel_{Mtb} activating complex. The addition of charged tRNA to this complex has the opposite effect by inhibiting transferase activity and activating hydrolysis activity. Differential control of Rel_{Mtb} gives the Mtb ribosomal complex a new regulatory role in controlling cellular metabolism in response to stringent growth conditions that may be present in the dormant Mtb lesion.

Mycobacterium tuberculosis (Mtb) infects more than one-third of the world's population, causes active disease in more than 16 million people, and kills more humans than any other bacterial pathogen. The extent of the problem is growing with the spread of AIDS, with the emergence of multi-drug-resistant strains, and with insufficient public health measures in widespread areas of the world. Most of the adult cases are the result of reactivation of an old, so-called dormant infection that had been controlled by a combination of the host immune response and bacterial adaptation. The details of the metabolic environment of a dormant Mtb lesion are not known, but are currently assumed to include oxygen limitation and nutrient source restriction (*1*). When microorganisms encounter an environment with limited nutrients, or other stress-related stimuli, many enter a dramatically slowed growth state characterized by a decrease in the levels of rRNA, tRNA, and protein synthesis, modified RNA polymerase activities, the diminished activity of many transport systems, and decreased carbohydrate, amino acid, and phospholipid metabolism (*2*). This is known as the stringent response and is mediated by the rapid accumulation of hyperphosphorylated guanosine, (p)ppGpp.[1] The stringent response is reversed when environmental conditions become favorable with the associated decrease in (p)ppGpp levels. The stringent response plays a role in the fruiting body development of *Myxococcus xanthus* (*3*), in regulating antibiotic production in *Streptomyces* (*4*), in the pathogenesis of *Legionella pneumophila* (*5*), and in the development of antibiotic resistance (*6*).

The RelA enzyme in *Escherichia coli* catalyzes the formation of pppGpp (*7*). The reaction involves a transfer of the 5′-β,γ-pyrophosphate group from ATP to the 3′-OH of GTP: ATP + GTP ↔ AMP + pppGpp (*8*). pppGpp is converted to ppGpp in *E. coli* by the action of a specific pppGpp 5′-γ-phosphohydrolase, encoded by the *gppA* gene (*9*), and ppGpp is believed to be the principal effector of the stringent response. The abbreviation (p)ppGpp is used to refer to both pppGpp and ppGpp.

Degradation of (p)ppGpp is catalyzed by the SpoT enzyme in *E. coli* (*10*). This enzyme encodes a (p)ppGpp 3′-pyrophosphohydrolase. In vitro, SpoT can hydrolyze the pyrophosphate group (PP_i) from the 3′-OH of both pppGpp and ppGpp, yielding GTP or GDP: (p)ppGpp ↔ GTP (GDP) + PP_i. The principal substrate for the hydrolysis reaction in vivo is believed to be ppGpp.

Unlike *E. coli*, in which (p)ppGpp is synthesized by the RelA protein and hydrolyzed by the SpoT protein, Mtb has one dual-function enzyme, Rel_{Mtb}, for both the synthesis and hydrolysis of (p)ppGpp (*11*). A strain of Mtb in which the gene encoding Rel_{Mtb} has been allelically disrupted does not

† This work was supported by NIH Grant AI43420 to H.R. D.A. is supported by the NIH Medical Scientist Training Program, and A.A. is supported by a Benjamin Franklin Scholar's research grant.

* To whom correspondence should be addressed: University of Pennsylvania, 225 Johnson Pavilion, Philadelphia, PA 19104. Telephone: (215) 662-6475. Fax: (215) 662-7842. E-mail: rubinh@mail.med.upenn.edu.

[1] Abbreviations: pppGpp, guanosine 5′-triphosphate, 3′-diphosphate; ppGpp, guanosine 5′-diphosphate, 3′-diphosphate; pppIpp, inosine 5′-triphosphate, 3′-diphosphate; aa-tRNA, aminoacyl-tRNA; $_{ox-red}$tRNA, tRNA which first has been oxidized with periodate and then reduced with borohydride; Phe-$tRNA^{Phe}$, phenylalanyl-$tRNA^{Phe}$; poly(U), poly(uridylic acid); poly(A), poly(adenylic acid); FPLC, fast performance liquid chromatography; PP_i, inorganic pyrophosphate; PEI, polyethylenimine.

10.1021/bi001256k CCC: $19.00
Published on Web 08/31/2000

make (p)ppGpp and is dramatically inhibited in its ability to survive in long-term cultures (*12*). We suggest that Rel_{Mtb} is a key factor in Mtb pathogenesis by regulating the intracellular concentrations of (p)ppGpp. Therefore, characterization of the opposing reactions of Rel_{Mtb} and their regulation is important in understanding adaption of Mtb to long-term survival and establishment of a dormant lesion.

MATERIALS AND METHODS

Enzyme. The pET22b expression system (Novagen) was used to purify the 82 kDa recombinant Rel_{Mtb} to homogeneity as previously described (*11*). The concentration of Rel_{Mtb} was determined with A_{280} (Beckman DU 640) using a calculated extinction coefficient of 0.979 for Rel_{Mtb} (Swiss-Prot Analysis).

Transferase Assays. Ribosome-independent transferase reaction mixtures (30 °C) contained 50 mM HEPES (pH 8.0), 100−225 mM NaCl, 1 mM DTT, the indicated concentrations of ATP and GTP (Pharmacia), 200 nM Rel_{Mtb}, and varying $MgCl_2$ or $MnCl_2$ concentrations. In addition, the Rel_{Mtb} activating complex reaction mixtures included ribosomes (0.15−0.30 μM), tRNA (0.20−1.50 μM), and mRNA [2.00 μM; poly(A) and poly(U) from Boehringer-Mannheim, poly(AU) from Sigma]. After the reaction components were mixed, the final pH was determined using an NMR pH electrode (Wilmad).

Assay Method 1. Reactions were monitored using either [γ-^{33}P]ATP or [γ-^{33}P]GTP (NEN) at 1 μCi/μmol. For consistent rates, radionucleotides were never used 10 days past their calibration date ($t_{1/2}$ = 25.4 days). Reaction rates were calculated by taking 5 μL aliquots at multiple time points, spotting on PEI-cellulose TLC plates (Sigma-Aldrich), and developing in 1.5 M KP_i (pH 3.4). Reaction products were visualized using a Storm Phosphorimager (Molecular Dynamics) with an enhanced sensitivity storage phosphor screen, and images were quantitated using ImageQuant version 1.2 (Molecular Dynamics). The identities of reaction products were confirmed using matrix-assisted laser desorption ionization (MALDI) mass spectroscopy (Wistar Institute). All reaction rates were linear with both time and enzyme concentration under these conditions, and less than 10% of the substrate was converted to product.

Assay Method 2. Large reaction volumes were set up. Aliquots were taken at multiple time points. Proteins were precipitated using 88% formic acid and centrifuged, and the supernatant containing the reaction products was analyzed using an ÄKTA FPLC system (Pharmacia) with a 1 mL Hi Trap anion exchange column (Pharmacia). The column was equilibrated using 20 mM Tris-HCl (pH 7.6) and 0.1 M NaCl and eluted with a linear gradient of 0.1 to 1.0 M NaCl; pppGpp elutes at 250 mM NaCl. Areas of the peaks corresponding to reactants (ATP and GTP) and products (AMP and pppGpp) were calculated using Unicorn Software version 2.11 (Pharmacia). Fitting of the kinetic equations used in this work to data was performed using a program for nonlinear regression analysis (*13*).

Assay for (p)ppGpp Hydrolysis. Hydrolysis reaction mixtures (30 °C) contained 50 mM HEPES (pH 8.0), 100−225 mM NaCl, 1 mM DTT, the indicated (p)ppGpp concentration, 200 nM Rel_{Mtb}, and varying $MnCl_2$ concentrations. Preparative amounts of pppGpp, ppGpp, pppIpp, and ppIpp were synthesized from partially purified purine nucleotide pyrophosphotransferase (PPK) from *Streptomyces morookaensis* (a gift from D. Gentry). *S. morookaensis* PPK was prepared as previously described (*11*). (p)ppGpp* was prepared in a reaction mixture containing 100 mM glycine (pH 10.0), 20 mM $MgCl_2$, [γ-^{33}P]ATP (15 mM, 1 μCi/μmol), 20 mM GTP, and 25 μL of PPK for 40 min at 37 °C. At the end of the incubation, the reaction mixture was brought to pH 7.0 using 1 N HCl, and (p)ppGpp was isolated using an ÄKTA FPLC system with a High Trap anion exchange column as described above. (p)ppGpp was dialyzed (100 Da molecular mass cutoff, Spectrum) to remove NaCl and lyophilized. The NaCl concentration in the (p)ppGpp preparation was measured using a Radiometer CDM210 conductivity meter. Concentrations of (p)ppGpp were determined spectrophotometrically using an ϵ_{252} of 1.37×10^4 M^{-1} cm^{-1}; the purity was confirmed by running on TLC with other nucleotide standards.

Assay 1. The hydrolysis reaction product,*PP_i, was visualized and quantitated as in Assay Method 1 for the transferase reaction.

Assay 2. PP_i was quantitated using a continuous spectrophotometric assay by following the decrease in A_{340} when 2 mol of NADH is oxidized to NAD^+ per mole of pyrophosphate consumed (*14*). A reagent consisting of coupled enzymatic reactions for the determination of pyrophosphate was purchased from Sigma. The reagent was reconstituted in 4 mL, bringing the reaction components to kinetically effective concentrations. Reaction mixtures (1 mL) were set up at 30 °C that contained 333 μL of the pyrophosphate reagent, 200 μL of the Rel_{Mtb} hydrolysis reaction mixture, and 467 μL of DDW. A blank mixture was set up that contained 333 μL of the pyrophosphate reagent and 667 μL of DDW to ensure that there was no decrease in A_{340} during the time course. Reaction mixtures containing known quantities of PP_i were run as standards to determine the decrease in A_{340} per nanomole of PP_i consumed. Consumption of 40 nmol of PP_i resulted in a decrease in A_{340} of approximately 0.4.

$$PP_i\ (\mu\text{mol/mL in sample}) = \frac{\Delta A_{Rel_{Mtb}\ \text{reaction}} - \Delta A_{\text{blank}}(\text{volume of reaction mixture in cuvette})}{6.22 \times 2 \times \text{volume of } Rel_{Mtb} \text{ reaction}}$$

where $\Delta A_{\text{RelMtb reaction}}$ = initial $A_{340Rel_{Mtb}\ \text{reaction}}$ − final $A_{340Rel_{Mtb}\ \text{reaction}}$, ΔA_{blank} = initial $A_{340\text{blank}}$ − final $A_{340\text{blank}}$, 6.22 is the millimolar absorbtivity of NADH at 340 nm, and 2 is the number of moles of β-NADH oxidized per mole of pyrophosphate consumed.

Ribosomes. Four liters of Mtb strain H37Rv and 4 L of *E. coli* strain Q13 (RNase−) were pelleted and resuspended in buffer A [10 mM Tris-HCl (pH 7.6), 30 mM KCl, 15 mM $MgCl_2$, and 6 mM β-mercaptoethanol]. Mtb was bead beaten; *E. coli* cells were French pressed to break open the cells, and 80 μg of DNase I was added to each. The cells were centrifuged at 15000*g* for 30 min, and the supernatant was recentrifuged at 30000*g* for 45 min. Puromycin was added to the supernatant to a final concentration of 0.1 mM and incubated at 37 °C for 20 min, and then centrifuged at 150000*g* for 3 h. The ribosome pellet was washed with buffer A, resuspended in buffer A, and layered over buffer B (buffer A with 30% w/v sucrose). This was centrifuged at 150000*g*

Table 1: Kinetic Constants for the Rel_{Mtb} Transferase Reaction[a]

reaction	K_{ATP} (mM)	K_{GTP} (mM)	k_{cat} (s^{-1})	k_{cat}/K_{ATP} (mM^{-1} s^{-1})	k_{cat}/K_{GTP} (mM^{-1} s^{-1})
(1) ribosome-independent transferase (Mg^{2+}) (basal level)	1.96 ± 0.24	1.38 ± 0.16	1.21 ± 0.16	0.62	0.88
(2) ribosome-independent transferase (Mn^{2+})	1.81 ± 0.23	1.27 ± 0.14	1.34 ± 0.19	0.74	1.05
(3) ribosome-independent transferase + uncharged tRNA (Mg^{2+})	1.08 ± 0.13	0.73 ± 0.12	1.28 ± 0.18	1.19	1.75
(4) ribosome-independent transferase + charged tRNA (Mg^{2+})	2.03 ± 0.26	1.48 ± 0.20	1.16 ± 0.17	0.57	0.78
(5) Rel_{Mtb} + the uncharged tRNA·ribosomes·mRNA (RAC) complex	0.45 ± 0.08	0.31 ± 0.06	24.68 ± 2.87	54.84	79.61
(6) Rel_{Mtb} + the charged tRNA·ribosomes· mRNA complex	1.73 ± 0.29	1.20 ± 0.18	1.46 ± 0.24	0.84	1.22

[a] The transferase reaction that was assayed was *p-p-p-A (*ATP) + p-p-p-G (GTP) ↔ p-A (AMP) + p-p-p-G-p-p*. p-p-p-G-p-p* indicates that the radioactive label is on the 3′-PP_i of the ribose ring of GTP. Reactions were performed at 30 °C and pH 8.0. For K_{ATP} determination, GTP was held constant at saturating levels (10−15 mM, 1 μCi/μmol of [γ-^{33}P]GTP); for K_{GTP} determination, ATP was held constant (10−15 mM, 1 μCi/μmol of [γ-^{33}P]ATP). These results were obtained using $tRNA^{Phe}$/poly(U). These experiments were also performed using $tRNA^{Lys}$/poly(A) and produced similar results. All assays were performed in triplicate at least two times.

for 15 h. The ribosome pellet was washed with buffer A, resuspended in buffer A, and centrifuged at 30000*g* for 45 min. The supernatant was layered over buffer B and centrifuged at 150000*g* for 18 h. The ribosome pellet was washed and resuspended in buffer C [50 mM Tris-HCl (pH 7.6), 50 mM KCl, and 10 mM $MgCl_2$] and centrifuged at 15000*g* for 45 min. The supernatant containing the ribosomes was stored at −80 °C. To quantitate the ribosomes and check the integrity of the 50S and 30S subunits, ribosomes were centrifuged through a 10 to 30% sucrose gradient without Mg^{2+}, and the gradient fractions were analyzed using an Isco UA-6 continuous UV reader. The ribosomes were quantitated using the conversion 1 A_{260} unit of 70S ribosomes = 25 pmol. The dependence of 50S and 30S subunit binding on Mg^{2+} concentration was determined by centrifuging isolated 70S ribosomes through a 10 to 30% sucrose gradient in the presence of different Mg^{2+} concentrations.

tRNA Synthetase. *E. coli* $tRNA^{Phe}$ synthetase was purified from DH5-α cells containing the cloned synthetase genes on plasmid pB1 (a gift from O. Uhlenbeck), according to the method of Peterson and Uhlenbeck (*15*). Purified $tRNA^{Tyr}$ synthetase from *Bacillus subtilis* and purified $tRNA^{Lys}$ synthetase from *Streptomyces aureus* were gifts from J. Tao. Crude Mtb tRNA synthetase was isolated according to the method of Deobagkar and Gopinathan (*16*).

tRNAs and tRNA Charging. One A_{260} unit of *E. coli* $tRNA^{Phe}$, $tRNA^{Lys}$, and $tRNA^{Tyr}$ (Sigma) represents 1200−1400 pmol of tRNA. $tRNA^{Phe}$, $tRNA^{Lys}$, and $tRNA^{Tyr}$ were charged under the following conditions: 50 mM HEPES (pH 7.5), 40 mM KCl, 14 mM $MgCl_2$, 0.5−10 μM tRNA, 50 μM ^{3}H-labeled amino acids, 20 nM pure synthetase or 2 μL of crude Mtb synthetase, 1 mM ATP, and 1 mM DTT for 25 min at 37 °C; these conditions were modified from published protocols to be compatible with the Rel_{Mtb} transferase−hydrolysis reactions. tRNA was first charged in a separate reaction using ^{3}H-labeled amino acids (NEN), and then added to the transferase−hydrolysis reactions. To confirm that ^{3}H-labeled aa-tRNA was completely charged before adding it to the transferase−hydrolysis reaction mixtures and that it remained charged throughout the course of the reactions, aliquots were spotted on Whatman 3MM paper and treated as previously described (*15*).

Biosensor Interaction Analysis. Kinetic and equilibrium constants for the interaction between Rel_{Mtb} and $tRNA^{Phe}$ were measured using a BIA2000 optical biosensor (Biacore Inc.) with simultaneous monitoring of four flow cells. Immobilization of Rel_{Mtb} to CM5 sensor chips was performed following the standard amine coupling procedure according to the manufacturer's specification. A blank reference surface (omission of protein ligand) and a BSA control were used as a background to correct instrument and buffer artifacts, and were generated at the same time under the same conditions. Binding experiments were performed at 25 °C in 10 mM HEPES (pH 7.4), 150 mM NaCl, and 0.005% Tween 20. $tRNA^{Phe}$ was dialyzed in this same buffer to reduce bulk flow effects. Association was assessed by passing tRNA over the chip surface at a flow rate of 30 μL/min for 1 min. The concentration range for the tRNA analyte was 2.5−40 μM, and the concentration of Rel_{Mtb} was 10 μM. Dissociation of bound analytes was monitored while the surface was washed with buffer for 2 min. Remaining analytes were removed from the surface by passing additional buffer over them for several minutes. Kinetic constants were obtained by global analysis with a 1:1 Langmuir binding model (A + B ↔ AB) with BIAcore evaluation software version 3.0. The equilibrium dissociation constant, K_d, was determined from ratios of k_{off}/k_{on}.

tRNA Modification. $NaIO_4$ oxidation followed by $NaBH_4$ reduction of tRNA ($_{ox-red}$tRNA) was carried out according to the method of Ofengand and Chen (*17*). This procedure specifically cleaves the C2−C3 bond of the ribose ring of the terminal adenosine without further modification of the tRNA.

Charged tRNA Isolation. The tRNA used in the deacylation reactions was first charged in a separate reaction, isolated using acid phenol (pH 4.5) extraction, and stored at −80 °C. After freezing and thawing, the [^{3}H]aa-tRNA was counted to ensure that it remained fully acylated.

RESULTS

Effects of Divalent Cations on Transferase and Hydrolysis Rates. To investigate how the opposing transferase and hydrolysis activities of Rel_{Mtb} are differentially regulated, each reaction was first studied separately in the absence of biological effectors. These reactions are termed the ribosome-independent reactions or the basal level of activity, and the mixtures contain only Rel_{Mtb} and either the transferase or hydrolysis substrates. The transferase reaction studied is ATP + GTP ↔ pppGpp + AMP. The catalytic constants for this reaction are shown in Table 1. Of eight divalent cations that were tested (Mn^{2+}, Mg^{2+}, Co^{2+}, Zn^{2+}, Cu^{2+}, Ni^{2+}, Fe^{2+}, and Ca^{2+}) only Mn^{2+} or Mg^{2+} supports the Rel_{Mtb} transferase reaction and only Mn^{2+} supports hydrolysis. Rel_{Mtb} has a very narrow metal concentration range required for maximum activity. The optimal Mg^{2+} concentration for the transferase reaction was approximately equal to the total concentration

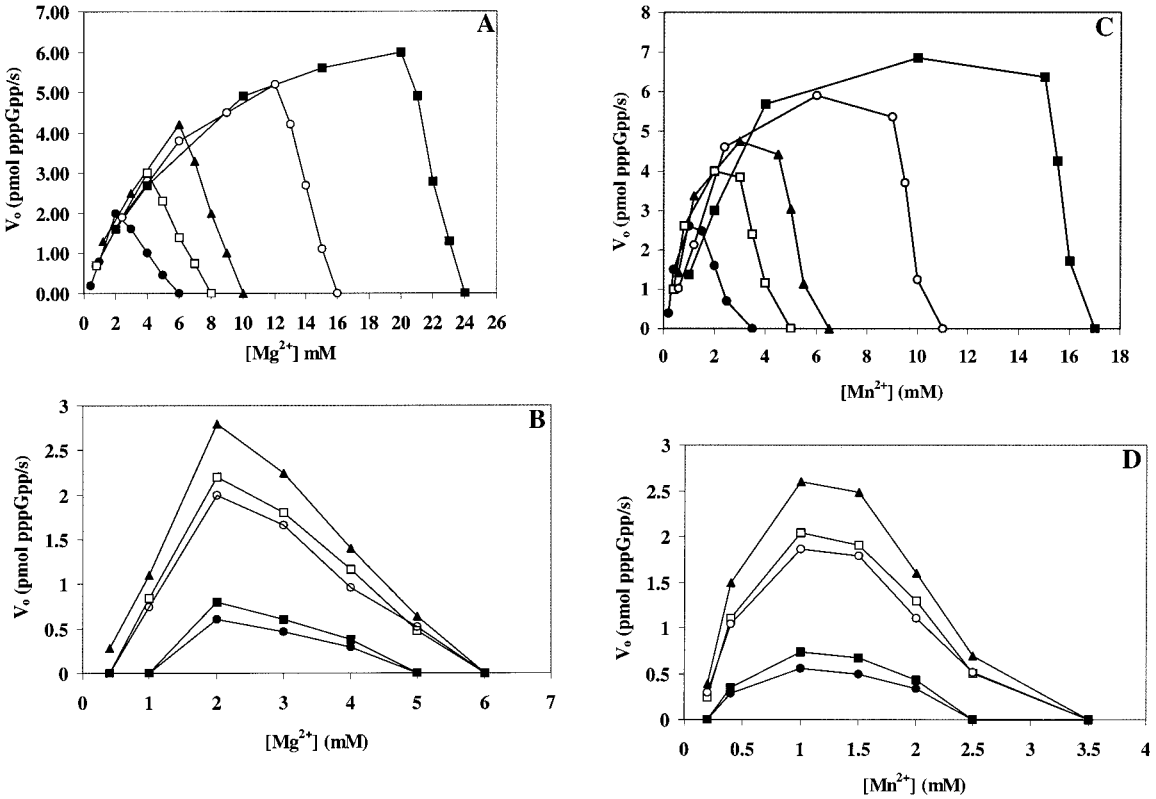

FIGURE 1: Dependence of the initial velocity (v_o) of Rel_{Mtb} transferase reaction on $[Mg^{2+}]$, $[Mn^{2+}]$, pH, and [ATP + GTP]. Reaction mixtures contained one of the following compounds at 50 mM: MOPS (pH 6.6−7.6), HEPES (pH 7.2−8.2), Tris-HCl (pH 7.2−8.8), CHES (pH 8.8−9.8), or CAPS (pH 9.8−10.8). (A) v_o as a function of $[Mg^{2+}]$ and 2 (●), 4 (□), 6 (▲), 12 (○), and 20 mM (■) ATP + GTP at a fixed pH (8.0). (B) v_o as a function of $[Mg^{2+}]$ at pH 7.2 (●), 7.7 (□), 8.2 (▲), 8.8 (○), and 9.5 (■) at a fixed substrate concentration (1 mM ATP + 1 mM GTP). (C) v_o as a function of $[Mn^{2+}]$ and 2 (●), 4 (□), 6 (▲), 12 (○), and 20 mM (■) ATP + GTP at a fixed pH (8.0). (D) v_o as a function of $[Mn^{2+}]$ at pH 7.2 (●), 7.7 (□), 8.2 (▲), 8.8 (○), and 9.5 (■) at a fixed substrate concentration (1 mM ATP + 1 mM GTP).

of nucleotide substrates, [ATP + GTP] (Figure 1A), whereas the optimal Mn^{2+} concentration was approximately one-half the total concentration of nucleotide substrates (Figure 1C). These metal requirements remained unchanged from pH 7.2 to 9.5 with maximal transferase rates occurring from pH 7.9 to 8.3 (Figure 1B,D). This contrasts with inorganic pyrophosphatase and thiamine pyrophosphokinase where there is a change in the optimal metal requirement with pH (*18*, *19*). Adding Mg^{2+} or Mn^{2+} in excess of NTP saturation decreased the Rel_{Mtb} transferase rate (Figure 1A,C). This decrease in rate is not due to an irreversible effect on the enzyme by the excess metal, because preincubation of Rel_{Mtb} with up to 6 mM Mg^{2+} or Mn^{2+} followed by dilution into assay buffer did not affect the rate of transferase activity.

Obtaining accurate rates for the transferase reaction in the presence of Mn^{2+}, where both transferase and hydrolysis reactions are active, is possible under initial velocity conditions, where the rate of pppGpp production greatly exceeds the rate of pppGpp hydrolysis. Therefore, only a very small fraction of pppGpp formed in the transferase reaction will be simultaneously hydrolyzed, allowing accurate quantitation of pppGpp.

The Rel_{Mtb}-catalyzed hydrolysis reaction is (p)ppGpp ↔ GTP (GDP) + PP_i. The catalytic constants for these reactions are shown in Table 2. The optimal Mn^{2+} concentration in the hydrolysis reaction was a 2−3-fold molar excess over the nucleotide substrate, (p)ppGpp (Figure 2A). As for the transferase reaction, this metal requirement remained unchanged from pH 7.2 to 9.5 with maximal hydrolysis activity occurring from pH 8.0 to 8.2 (Figure 2B). At all (p)ppGpp concentrations that were tested, adding Mn^{2+} in excess of its optimal concentration decreased the rate of hydrolysis (Figure 2A). Again, preincubation of Rel_{Mtb} with up to 6 mM free Mn^{2+}, followed by dilution into assay buffer, did not affect the hydrolysis rate. Mg^{2+} alone could not activate hydrolysis, nor were there any synergistic effects on rates when Mn^{2+} and Mg^{2+} were combined. Adding a vast excess of Mg^{2+} (20 mM) did not inhibit Rel_{Mtb} hydrolysis activity, while even a small concentration of free Mg^{2+} inhibited transferase activity.

Simultaneous Catalysis of Rel_{Mtb} Ribosome-Independent Transferase and Hydrolysis Reactions. The differential sensitivity of the two reactions to Mg^{2+} suggested that there are two independent catalytic sites for hydrolysis and synthesis of (p)ppGpp.

To further study whether the transferase and hydrolysis reactions of Rel_{Mtb} are catalyzed at the same active site or distinct active sites, it was tested whether the two reactions could be catalyzed simultaneously. The transferase and hydrolysis reactions were first carried out separately in identical buffer, pH, and NaCl and Mn^{2+} concentration conditions (Mn^{2+} concentration based on the concentration of nucleotides used). In reactions A1−D1, the concentrations of transferase and hydrolysis substrate added are close to the K_m. In reactions A2−D2, the concentrations of the added transferase substrates are approximately 3-fold greater than K_m, and the concentration of the added hydrolysis substrate is approximately 7-fold greater than K_m. For example, in

Table 2: Kinetic Constants for the Rel_{Mtb} Hydrolysis Reaction[a]

reaction	K_m (mM)	k_{cat} (s^{-1})	k_{cat}/K_m (mM^{-1} s^{-1})
(1) Rel_{Mtb} + pppGpp (basal level)	0.48 ± 0.06	2.83 ± 0.33	5.90
(2) Rel_{Mtb} + pppGpp + uncharged tRNA	1.21 ± 0.13	1.56 ± 0.24	1.29
(3) Rel_{Mtb} + pppGpp + charged tRNA	0.61 ± 0.09	2.61 ± 0.40	4.28
(4) Rel_{Mtb} + pppGpp + the uncharged tRNA·ribosomes·mRNA complex	1.42 ± 0.17	1.41 ± 0.28	0.99
(5) Rel_{Mtb} + pppGpp + the charged tRNA·ribosomes·mRNA complex	0.69 ± 0.11	2.91 ± 0.38	4.22
(6) Rel_{Mtb} + ppGpp (basal level)	0.41 ± 0.06	2.97 ± 0.32	7.24
(7) Rel_{Mtb} + ppGpp + uncharged tRNA	1.13 ± 0.14	1.41 ± 0.25	1.25
(8) Rel_{Mtb} + ppGpp + charged tRNA	0.52 ± 0.08	2.68 ± 0.41	5.15
(9) Rel_{Mtb} + ppGpp + the uncharged tRNA·ribosomes·mRNA complex	1.33 ± 0.15	1.30 ± 0.25	0.98
(10) Rel_{Mtb} + ppGpp + the charged tRNA·ribosomes·mRNA complex	0.59 ± 0.11	2.98 ± 0.35	5.05
(11) Rel_{Mtb} + pppIpp	no activity	no activity	
(12) Rel_{Mtb} + ppIpp	no activity	no activity	

[a] The hydrolysis reaction that was assayed was either (1) p-p-p-G-p-p* (pppGpp) ↔ *PP_i + p-p-p-G (GTP) (where p-p-p-G-p-p* indicates that the radioactive label is on the 3′-PP_i of the ribose ring of GTP) or (2) p-p-G-p-p* (ppGpp) ↔ *PP_i + p-p-G (GDP) (where p-p-G-p-p* indicates that the radioactive label is on the 3′-PP_i of the ribose ring of GTP). Reactions were performed at 30 °C and pH 8.0. These results were obtained using $tRNA^{Phe}$/poly(U). These experiments were also performed using $tRNA^{Lys}$/poly(A) and produced similar results. All assays were performed in triplicate at least two times.

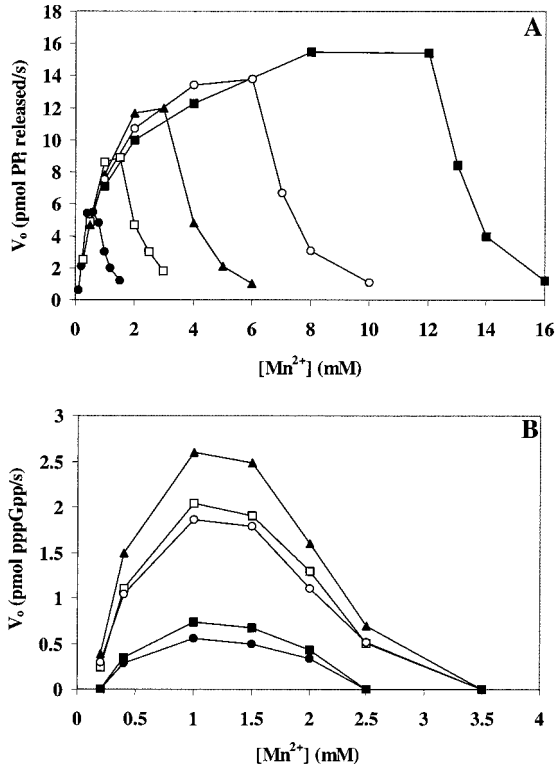

FIGURE 2: Dependence of the initial velocity (v_o) of Rel_{Mtb} hydrolysis reaction on [Mn^{2+}], pH, and [pppGpp]. (A) v_o as a function of [Mn^{2+}] and 0.2 (●), 0.5 (□), 1 (▲), 2 (○), and 4 mM (■) pppGpp at a fixed pH (8.0). (B) v_o as a function of [Mn^{2+}] at pH 7.2 (●), 7.7 (□), 8.2 (▲), 8.8 (○), and 9.5 (■) at a fixed substrate concentration (0.3 mM pppGpp).

reaction A1 [50 mM HEPES (pH 8.0), 150 mM NaCl, 1 mM DTT, 1.4 mM Mn^{2+}, 1 mM *ATP, 1 mM GTP, and 200 nM Rel_{Mtb}], the ribosome-independent transferase activity reaches its maximum rate for this concentration of *ATP + GTP (Table 3). In reaction B1 [50 mM HEPES (pH 8.0), 150 mM NaCl, 1 mM DTT, 1.4 mM Mn^{2+}, 0.7 mM pppGpp*, and 200 nM Rel_{Mtb}], the hydrolysis activity reaches its maximum rate for this concentration of pppGpp* (Table 3). It was then tested whether both transferase and hydrolysis could be carried out at their maximum rates simultaneously in the presence of substrates for both reactions. Two reactions were set up, C1 and D1, each reaction mixture containing substrate for both transferase and hydrolysis reactions (Table 3). Reaction mixture C1 contained 50 mM HEPES (pH 8.0), 150 mM NaCl, 1 mM DTT, 1 mM *ATP, 1 mM GTP, 0.7 mM pppGpp, 200 nM Rel_{Mtb}, and 2.8 mM Mn^{2+}. The radioactive label on *ATP allowed the transferase rate to be monitored in the presence of the added pppGpp. Reaction mixture D1 contained 50 mM HEPES (pH 8.0), 150 mM NaCl, 1 mM DTT, 1 mM ATP, 1 mM GTP, 0.7 mM pppGpp*, 200 nM Rel_{Mtb}, and 2.8 mM Mn^{2+}. The radioactive label on pppGpp* allowed the hydrolysis rate to be monitored in the presence of the added ATP and GTP. Under these conditions, both the transferase and hydrolysis reactions were catalyzed simultaneously at their maximal rates (Table 3). This example holds true for a range of nucleotide concentrations tested in the simultaneous reactions (Table 3, reactions A2−D2). The data from these simultaneous transferase and hydrolysis reactions were obtained under initial velocity conditions. Under these conditions, the amount of pppGpp generated during the transferase reaction (<0.1 mM) is small compared to the amount of pppGpp added to assay hydrolysis (0.7 mM), so it will not increase the rate of the hydrolysis reaction. Likewise, under initial velocity conditions, the amount of GTP generated by the hydrolysis of pppGpp (<0.1 mM) is small compared to the amount of GTP added to assay transferase (1.0 mM), so it will not increase the rate of the transferase reaction.

An additional observation supporting the existence of two active sites is that (p)ppIpp can be synthesized but cannot be hydrolyzed by Rel_{Mtb}, indicating a second active site that is specific for (p)ppGpp hydrolysis (Table 2).

Higher-Level Regulation of Rel_{Mtb} Activities and Effects of Uncharged tRNA. The problem of differential regulation of the synthesis and degradation of (p)ppGpp is resolved in some microorganisms by encoding these activities on different enzymes. In *E. coli*, RelA synthesis of (p)ppGpp is activated by binding uncharged tRNA to the A-site of a ribosome that is stalled on a codon for which there are no cognate aa-tRNAs (*20*). *E. coli* SpoT hydrolysis of (p)ppGpp is not activated by a ribosome complex (*10*). Therefore, the role of the ribosome, tRNA, and mRNA in the regulation of Rel_{Mtb} synthesis and degradation of (p)ppGpp was investigated. Ribosomes were prepared from Mtb and *E. coli*. The availability of purified, specific Mtb tRNAs is limited, so highly purified, codon-specific *E. coli* tRNAs were used. The three *E. coli* tRNAs used in these experiments ($tRNA^{Phe}$, $tRNA^{Lys}$, and $tRNA^{Tyr}$) were efficiently charged using crude Mtb tRNA synthetase, suggesting tRNA structures similar

Table 3: Simultaneous Catalysis of the Rel_{Mtb} Transferase and Hydrolysis Reactions[a]

reaction	transferase rate (pmol/s)	hydrolysis rate (pmol/s)
(A1) Rel_{Mtb} + 1.0 mM *ATP + 1.0 mM GTP	2.20 ± 0.16	
(B1) Rel_{Mtb} + 0.7 mM pppGpp*		9.68 ± 0.73
(C1) Rel_{Mtb} + 1.0 mM *ATP + 1.0 mM GTP + 0.7 mM pppGpp	2.07 ± 0.19	not monitored
(D1) Rel_{Mtb} + 1.0 mM ATP + 1.0 mM GTP + 0.7 mM pppGpp*	not monitored	9.17 ± 0.77
(A2) Rel_{Mtb} + 5.0 mM *ATP + 5.0 mM GTP	5.43 ± 0.42	
(B2) Rel_{Mtb} + 3.5 mM pppGpp*		14.96 ± 1.23
(C2) Rel_{Mtb} + 5.0 mM *ATP + 5.0 mM GTP + 3.5 mM pppGpp	5.11 ± 0.47	not monitored
(D2) Rel_{Mtb} + 5.0 mM ATP + 5.0 mM GTP + 3.5 mM pppGpp*	not monitored	14.45 ± 1.36
(A3) Rel_{Mtb} + RAC + 1 mM *ATP + 1 mM GTP	76.24 ± 5.15	
(B3) Rel_{Mtb} + RAC + 0.7 mM pppGpp*		3.39 ± 0.28
(C3) Rel_{Mtb} + RAC + 1.0 mM *ATP + 1.0 mM GTP + 0.7 mM pppGpp	73.05 ± 5.88	not monitored
(D3) Rel_{Mtb} + RAC + 1.0 mM ATP + 1.0 mM GTP + 0.7 mM pppGpp*	not monitored	1.75 ± 0.16
(A4) Rel_{Mtb} + RAC + 5.0 mM *ATP + 5.0 mM GTP	121.42 ± 8.46	
(B4) Rel_{Mtb} + RAC + 3.5 mM pppGpp*		6.53 ± 0.48
(C4) Rel_{Mtb} + RAC + 5.0 mM *ATP + 5.0 mM GTP + 3.5 mM pppGpp	116.23 ± 7.49	not monitored
(D4) Rel_{Mtb} + RAC + 5.0 mM ATP + 5.0 mM GTP + 3.5 mM pppGpp*	not monitored	3.44 ± 0.26

[a] The location of the radioactive label is indicated with an asterisk. Reactions including nonradioactive substrates were not monitored. Reactions were performed at 30 °C and pH 8.0. The NaCl concentration was normalized in reactions A−D to account for the increased NaCl added by the (p)ppGpp or ATP/GTP stocks. The RAC consisted of $tRNA^{Phe}$, ribosomes, and poly(U).

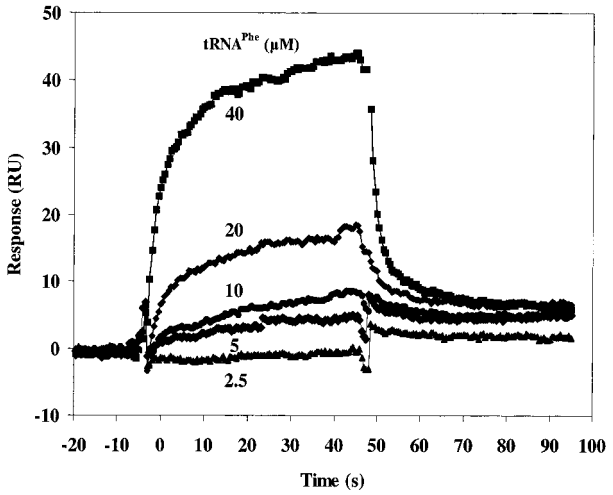

FIGURE 3: Biosensor interaction analysis of tRNA binding to Rel_{Mtb}. Sensorgram overlays showing binding of various concentrations of $tRNA^{Phe}$ to Rel_{Mtb} immobilized on the sensor surface. Concentrations of $tRNA^{Phe}$ are shown next to each sensorgram. The surface density was 80 RUs; the buffer was 10 mM HEPES (pH 7.4), 150 mM NaCl, and 0.005% Tween. An increase in response reflects binding of $tRNA^{Phe}$. The subsequent signal decay shows dissociation of bound $tRNA^{Phe}$ upon washing with running buffer alone. The lines through the experimental data show global fits of association and dissociation phases using a 1:1 Langmuir binding model in BIAcore evaluation software version 3.0.

to their Mtb tRNA homologues. In addition, *E. coli* $tRNA^{Ile}$ (*21*) and $tRNA^{Met}$ (*22*) have been charged by purified Mtb synthetases. It was reported previously that Rel_{Mtb} complements a RelA/SpoT double mutant of *E. coli* (*11*), again indicating the conserved nature of certain aspects of components of the translation complexes of *E. coli* and Mtb.

Adding uncharged tRNA alone to the Rel_{Mtb} ribosome-independent transferase reaction caused a 2-fold decrease in K_{ATP} and K_{GTP}, but did not increase k_{cat} (Table 1, reaction 1 vs 3). This modest effect on Rel_{Mtb} would be consistent with low-affinity binding of uncharged tRNA to Rel_{Mtb}, and this was confirmed by biosensor interaction analysis, which yielded a K_d of 2.8×10^{-5} M, a k_{on} of 9.6×10^2 M^{-1} s^{-1}, and a k_{off} of 2.7×10^{-2} s^{-1} (Figure 3). However, adding uncharged tRNA to the hydrolysis reaction mixture increased the K_m and decreased the k_{cat} for (p)ppGpp (Table 2, reaction 1 vs 2), which our data indicate occurs at a site different than the transferase site.

Adding a complex of uncharged tRNA, ribosomes, and cognate mRNA to the transferase reaction mixture lowered K_{ATP} and K_{GTP} 4-fold and increased k_{cat} 20-fold, resulting in a substantial increase in k_{cat}/K_m (Table 1, reaction 1 vs 5). Activation of the Rel_{Mtb} transferase reaction depends on the formation of the Rel_{Mtb}·uncharged tRNA·ribosome·mRNA quarternary complex, which we term the Rel_{Mtb} activating complex for (p)ppGpp synthesis or RAC. Omission of any component from the RAC resulted in no activation of the transferase reaction over basal levels (Table 4, reactions 4−6), and the addition of tRNA, ribosomes, and mRNA without Rel_{Mtb} gave no detectable transferase activity. Furthermore, substituting a noncognate tRNA·mRNA pair resulted in no activation (Table 4, reaction 10).

To determine if uncharged tRNA activates Rel_{Mtb} by entering the A-site of the ribosome or whether it activates Rel_{Mtb} independently of the ribosome or by interaction at another site on the ribosome, tetracycline was added to the RAC reaction mixture. Tetracycline interrupts elongation of polypeptide chains by preventing tRNA from entering the A-site of the ribosome. Tetracycline was first added at concentration ranging from 20 to 500 μM to the Rel_{Mtb} ribosome-independent transferase reaction mixture and had no effect on the reaction rate, indicating that tetracycline does not inhibit Rel_{Mtb} activity directly (data not shown). Tetracycline was then added at a concentration of 20 μM to the RAC reaction, and it completely inhibited the activation of Rel_{Mtb} by blocking the entry of uncharged tRNA into the A-site of the ribosome (Table 4, reaction 9).

Higher concentrations of Mg^{2+} were required in the RAC reaction than in the ribosome-independent reaction because assembly of the RAC was optimal at approximately 14 mM Mg^{2+}; additional Mg^{2+} was then needed to coordinate the nucleotides, as in the ribosome-independent reaction. For example, assaying transferase activity with 1 mM ATP and 1 mM GTP required 16 mM Mg^{2+} (14 mM Mg^{2+} to assemble the RAC with 2 mM Mg^{2+} to coordinate the nucleotides), while 3 mM ATP and 3 mM GTP required 20 mM Mg^{2+} for optimal activity. Unlike the ribosome-independent transferase reaction, the presence of high concentrations of free Mg^{2+} in the RAC reaction did not

Table 4: Activation of the Rel_{Mtb} Transferase Reaction Requires the RAC Quarternary Complex[a]

reaction	v_o (pmol/s)
(1) Rel_{Mtb} ribosome-independent transferase (basal level)	1.0 (normalized)
(2) Rel_{Mtb} + $tRNA^{Phe}$	2.2
(3) Rel_{Mtb} + Phe-$tRNA^{Phe}$	1.3
(4) Rel_{Mtb} + the $tRNA^{Phe}$·ribosomes complex	1.6
(5) Rel_{Mtb} + the $tRNA^{Phe}$·poly(U) complex	1.8
(6) Rel_{Mtb} + the ribosomes·poly(U) complex	0.9
(7) Rel_{Mtb} + the $tRNA^{Phe}$·ribosomes·poly(U) complex	21.8
(8) Rel_{Mtb} + the Phe- $tRNA^{Phe}$·ribosomes·poly(U) complex	1.2
(9) Rel_{Mtb} + the $tRNA^{Phe}$·ribosomes·poly(U) complex + tetracycline	1.3
(10) Rel_{Mtb} + the $tRNA^{Phe}$·ribosomes·poly(A) complex	1.5
(11) Rel_{Mtb} + the $tRNA^{Phe}$·ribosomes·poly(U) complex + Lys-$tRNA^{Lys}$	20.3
(12) Rel_{Mtb} + the $_{ox-red}tRNA^{Phe}$·ribosomes·poly(U) complex	1.5

[a] All rates (v_o) were obtained at 30 °C, pH 8.0, 1 mM ATP, and 1 mM GTP. Ribosomes were present at 0.2 μM; $tRNA^{Phe}$ was present at 1.2 μM and poly(U) or poly(A) at 2.0 μM. These experiments were also performed with $tRNA^{Lys}$ and $tRNA^{Tyr}$. The final concentration of tetracycline was 20 μM.

inhibit transferase activity, suggesting that the RAC exerts a structural constraint on Rel_{Mtb}, locking it into an active conformation.

As a further step toward understanding the mechanism by which uncharged tRNA activates Rel_{Mtb}, the C2−C3 bond of the ribose ring on the terminal adenosine of $tRNA^{Phe}$ and $tRNA^{Lys}$ was cleaved by treatment with periodate and then borohydride (*17*). This procedure forms an unoriented diol ester which, for example, cannot bind to EF-Tu (*17*). The $_{ox-red}$tRNA·ribosomes·mRNA complex failed to activate Rel_{Mtb} transferase activity over basal levels (Table 4, reaction 12), indicating that the unoriented hydroxyl groups of the terminal adenosine were no longer able to either participate directly in the reaction mechanism or induce a conformational change in Rel_{Mtb}.

Additional fine-tuning of (p)ppGpp levels is accomplished by the RAC inhibiting the hydrolytic activity of Rel_{Mtb} (Table 2); the K_m for (p)ppGpp is increased and the k_{cat} decreased, reducing k_{cat}/K_m from 5.9 to 0.99 mM^{-1} s^{-1} for pppGpp hydrolysis (reaction 1 vs 4) and the k_{cat}/K_m from 7.24 to 0.98 mM^{-1} s^{-1} for ppGpp hydrolysis (reaction 6 vs 9).

Higher-Level Regulation of Rel_{Mtb} Activities and Effects of Charged tRNA. If differential regulation of Rel_{Mtb} reflects the level of available amino acids and the ratio of uncharged to charged tRNA in the cell, then charged tRNA might either inhibit or simply fail to activate Rel_{Mtb} transferase activity. To test these possibilities, tRNA was aminoacylated in a separate reaction mixture and added to the transferase reaction mixture along with its tRNA synthetase to continually regenerate charged tRNA. In the ribosome-independent transferase reaction, the addition of charged tRNA alone decreased the k_{cat}/K_m for both substrates, ATP and GTP, compared to adding uncharged tRNA (Table 1, reaction 4 vs 3). Furthermore, adding a charged tRNA·ribosomes·mRNA complex to Rel_{Mtb} fails to activate (p)ppGpp synthesis, resulting in significantly lower k_{cat}/K_m values relative to that of the RAC reaction (Table 1, reaction 6 vs 5).

The cellular ratio of uncharged tRNA to charged tRNA increases as the microbial environment is depleted in amino acids. This situation was re-created in vitro by adding Phe-$tRNA^{Phe}$ to the RAC transferase reaction mixture in the absence of phenylalanyl-tRNA synthetase, which results in complete Phe-$tRNA^{Phe}$ deacylation by the end of the transferase reaction. Figure 4A indicates that as Phe-$tRNA^{Phe}$ starts to deacylate and the ratio of $tRNA^{Phe}$ to Phe-$tRNA^{Phe}$ increases, the rate of (p)ppGpp production approaches V_{max}. Therefore, inhibition of Rel_{Mtb} activity by charged tRNA is

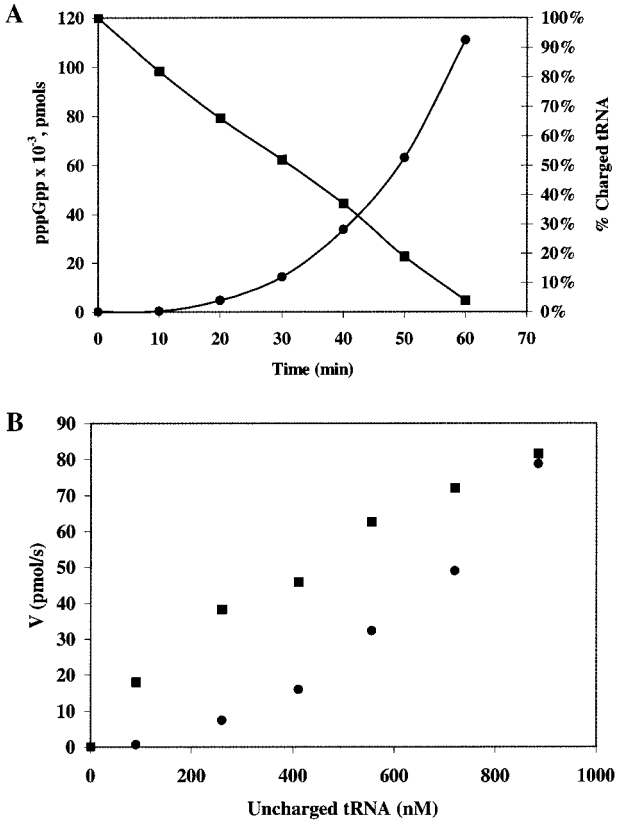

FIGURE 4: Inhibition of Rel_{Mtb} transferase activity by charged tRNA. (A) pppGpp formation as a function of Phe-$tRNA^{Phe}$ deacylation. [^{3}H]Phe-$tRNA^{Phe}$ (1.0 μM) that had been separated from phenylalanyl-tRNA synthetase was added to the RAC transferase reaction mixture. Reaction mixtures contained 0.2 μM poly(U)-programmed ribosomes. Deacylation of [^{3}H]Phe-$tRNA^{Phe}$ was monitored by scintillation counting, and the percentage of the charged tRNA remaining at each time point is indicated on the *Y*-axis (■); transferase activity was monitored by detecting [^{33}P]pppGpp (●). (B) Comparison of RAC transferase rates in the presence and absence of charged tRNA. Transferase rates of reactions with both charged and uncharged tRNA were calculated for 10 min intervals from the progress curve depicted in panel A. The concentration of uncharged tRNA during the 10 min intervals was taken as the average amount of uncharged tRNA formed during this time period. These data (●) were plotted against transferase rates obtained by adding different concentrations of uncharged tRNA in the absence of charged tRNA (■).

reversible upon deacylation. Differentiating the progress curve for pppGpp production in Figure 4A indicates that transferase rates are lower in reaction mixtures that contain both charged and uncharged tRNA·ribosomes·mRNA com-

plexes than in reaction mixtures that contain only the uncharged tRNA·ribosomes·mRNA complex (Figure 4B). This is consistent with previous reports that both uncharged and charged tRNA have an equal affinity for the ribosomal A-site (*23*). Charged tRNA may not interact directly with Rel_{Mtb} to inhibit transferase activity; it may block the A-site of the ribosome and prevent the activator, uncharged tRNA, from directly activating Rel_{Mtb}.

To confirm that charged tRNA was not inhibiting Rel_{Mtb} transferase activity independently of the ribosome and was not exerting its effects at a site other than the A-site of the ribosome, Lys-$tRNA^{Lys}$ was added to the $tRNA^{Phe}$·ribosome·poly(U)·Rel_{Mtb} activating complex. Activation of Rel_{Mtb} by A-site-bound $tRNA^{Phe}$ was not inhibited by the presence of Lys-$tRNA^{Lys}$, because Lys-$tRNA^{Lys}$ is unable to enter the A-site of the ribosome in the absence of its cognate mRNA template (Table 4, reaction 11).

Adding the charged tRNA·ribosomes·mRNA complex or charged tRNA alone to the Rel_{Mtb} hydrolysis reaction mixture causes no change in the K_m or k_{cat} for (p)ppGpp relative to basal levels (Table 2, reactions 3 and 5 vs 1 and reactions 8 and 10 vs 6), raising the possibility that Rel_{Mtb}-catalyzed hydrolysis of (p)ppGpp may occur while the enzyme is bound to the ribosome or free in the cytoplasm.

Simultaneous Catalysis of RAC Transferase and Hydrolysis Reactions. The data in Table 3 (reactions A1−D1 and A2−D2) indicate that in the absence of biological control elements (the RAC), Rel_{Mtb} transferase and hydrolysis reactions can be catalyzed simultaneously at their maximum rates. These simultaneous transferase−hydrolysis experiments were repeated for the RAC reactions (Table 3). Adding hydrolysis substrate (p)ppGpp did not lower transferase rates in the RAC reaction (Table 3, A3 vs C3 and A4 vs C4). However, when hydrolysis is assayed in the presence of the RAC and the absence of transferase substrate ATP or GTP, hydrolysis rates are decreased by 55−65% relative to basal levels (Table 3, B1 vs B3 and B2 vs B4). Furthermore, adding ATP and GTP, in addition to the RAC, to the hydrolysis reaction mixture results in an additional 50% decrease in the hydrolysis rate (Table 3, B3 vs D3 and B4 vs D4). The proposed RAC-induced conformational change in Rel_{Mtb} results in tighter binding of ATP and GTP to the transferase active site (Table 1) and further inhibits the (p)ppGpp hydrolysis reaction.

DISCUSSION

Our studies indicate that the differential regulation of the opposing activities of Rel_{Mtb} is a complex function of divalent cation concentration and the aminoacylation state of a tRNA·ribosome·mRNA complex. This ability to rapidly fine-tune cellular (p)ppGpp concentration in response to available nutrients is essential for the long-term survival of Mtb. Without efficient regulation of Rel_{Mtb}, there would be unnecessary cycling of its substrates, ATP and GTP. This cycling would result in a drastic reduction in the size of the available pool of high-energy compounds necessary for cellular function.

Like all pyrophosphate transfer enzymes, Rel_{Mtb} activity is dependent on divalent cations. The optimal Mg^{2+} concentration for the ribosome-independent transferase reaction was approximately equal to the total concentration of nucleotide substrates, [ATP + GTP] (Figure 1A), whereas the optimal Mn^{2+} concentration was approximately one-half the total concentration of nucleotide substrates (Figure 1C). Under these transferase reaction conditions, 85% of the Mg^{2+} and 99% of the Mn^{2+} are nucleotide-bound, assuming dissociation constants of 50 and 10 μM for Mg^{2+}-NTP and Mn^{2+}-NTP, respectively (*24*). Unless there are very tight metal binding sites on the enzyme, or binding of the metal−nucleotide substrate to Rel_{Mtb} significantly lowers the K_d of the enzyme for the metal as is the case for MutT (*24*), very little metal will be enzyme-bound. Only eight enzymes have been identified that catalyze the transfer of a pyrophosphate group via nucleophilic substitution at the β-phosphorus rather than the more common substitution at the α-phosphorus (*25*). The Rel class of enzymes is included in this family (*25*). It has been shown for all but the Rel class by kinetic or metal binding studies that these enzymes utilize a dual-divalent cation mechanism, with one metal coordinating the substrate and a second metal bound to the enzyme. In a dual-divalent mechanism, the concentration of divalent cation needed for optimal enzyme activity well exceeds that necessary for saturation of nucleotide substrate, leaving high enough concentrations of free metal to bind to the enzyme. However, for Rel_{Mtb}, adding Mg^{2+} or Mn^{2+} in excess of NTP saturation caused a severe decrease in the transferase rate (Figure 1A,C).

There may be low-affinity Mg^{2+} binding sites in the transferase active site, and binding of excess metal to these weak Mg^{2+} sites may change the enzyme's conformation and reduce transferase activity. A similar metal requirement has been reported for DNA polymerase I, which has an enzymatic mechanism involving nucleotidyl transfer with pyrophosphate release (*26*). In the presence of the RAC, Rel_{Mtb} transferase activity is not inhibited by free Mg^{2+}, indicating that the RAC constrains the structure of Rel_{Mtb}. The hydrolysis active site may not have low-affinity Mg^{2+} binding sites, which would explain why the hydrolysis rate is not decreased by free Mg^{2+}. Therefore, we conclude that Rel_{Mtb}-mediated pyrophosphoryl transfer may be an example of an attack at the β-phosphorus not requiring a dual-divalent cation mechanism.

Rel_{Mtb} is a member of the superfamily of single-gene-encoded bifunctional enzymes that catalyze opposing reactions which include (1) the family of histidine kinases and phosphatases (*27*), (2) the adenylyl transferase (ATase) and uridylyl transferase (UTase) system (*28*), (3) glutathionylspermidine synthetase (*29*), (4) 6-phosphofructo-2-kinase or fructose 2,6-bisphosphatase (*30*), and (5) isocitrate dehydrogenase kinase or phosphatase (*31*). The bifunctionality of systems 1−4 arises from two independent active sites on the enzyme, whereas it is believed that IDH kinase or phosphatase contains only one active site and the kinase back reaction gives rise to the phosphorylase activity (*31*). Whereas the bifunctionality of some of these enzymes appears to be a consequence of covalent modification, e.g., phosphorylation or proteolysis, it appears that Rel_{Mtb} is regulated in an allosteric manner.

The formation of a stable, enzymatically active, ribosomal structure has also been described for (1) the GTPase activation of eRF3 in the presence of eRF1 and ribosomes

(*32*), (2) the stimulation of EF-G GTPase activity by tRNA in the ribosomal P-site (*33*), and (3) the GTPase state of the EF-Tu·aa-tRNA·GTP complex and proper codon recognition in the presence of ribosomes (*34*). When the EF-Tu·aa-tRNA·GTP complex binds to the ribosome, cognate codon−anticodon interaction leads to a conformational change in tRNA that is transmitted to EF-Tu, triggering GTPase activity. Rel_{Mtb} transferase may be activated by a conformational change in uncharged tRNA that occurs upon entry into the A-site, resulting in a productive interaction between the terminal adenosine of tRNA and Rel_{Mtb}. This is consistent with the observations that adding uncharged tRNA alone to Rel_{Mtb} results in weak transferase activation, and formation of the RAC is inhibited by tetracycline, which prevents tRNA from entering the A-site (Table 4). However, unlike EF-Tu activation where a structural change in charged tRNA associated with codon−anticodon recognition is transmitted to the G domain, a RAC is not formed if uncharged tRNA is replaced by charged tRNA. This indicates that in addition to the tRNA conformational changes caused by codon−anticodon interactions, Rel_{Mtb} activation is also dependent on the aminoacylation state of tRNA.

In the absence of biological control factors, Rel_{Mtb} can simultaneously synthesize (p)ppGpp and hydrolyze (p)ppGpp at each reaction's optimal rate. However, in the presence of the RAC regulatory system, there is a substantial increase in transferase activity yet a significant reduction in hydrolysis activity. Furthermore, the presence of transferase substrates and the RAC causes an almost complete shutdown of hydrolysis activity. Therefore, we propose that the RAC lowers the K_m of the transferase substrates, triggering an allosteric effect that is communicated to the hydrolysis active site.

Thus, the differential control of Rel_{Mtb} by the RAC is mediated by the conformational changes of the two distinct active sites as a function of the state of tRNA aminoacylation. A more refined model will depend on determining the role that the local ribosomal protein, rRNA, and tRNA environment around Rel_{Mtb} plays in regulating its activity. These studies will be facilitated by the emerging high-resolution structures of ribosomes (*35*) and future work on the structure of Rel_{Mtb}.

ACKNOWLEDGMENT

MALDI analysis was performed at the Wistar Institute. We thank the University of Pennsylvania Biosensor Interaction Analysis Core Facility for assistance with Biosensor experiments and Dr. Lin-Sheng Li for excellent technical assistance. We thank Drs. Michael Cashel, Dan Gentry, Olke Uhlenbeck, Clifton Barry, and Jianshi Tao for their valuable reagents and helpful discussions.

REFERENCES

1. Cunningham, A. F., and Spreadbury, C. L. (1998) *J. Bacteriol. 180*, 801.
2. Cashel, M., Gentry, D. R., Hernandez, V. J., and Vinella, D. (1996) In *Escherichia coli and Salmonella: Cellular and Molecular Biology* (Neidhardt, F. C., Curtis, R., Ingraham, J. L., Lin, E. C. C., Low, K. B., Magasanik, B., Reznikoff, W. S., Riley, M., Schaechter, M., and Umbarger, H. E., Eds.) ASM Press, Washington, DC.
3. Harris, B. Z., Kaiser, D., and Singer, M. (1998) *Genes Dev. 12*, 1022.
4. Martinez-Costa, O. H., Arias, P., Romero, N. M., Parro, V., Mellado, R. P., and Malpartida, F. (1996) *J. Biol. Chem. 271*, 10627.
5. Hammer, B. K., and Swanson, M. S. (1999) *Mol. Microbiol. 33*, 721.
6. Greenway, D. L., and England, R. R. (1999) *Lett. Appl. Microbiol. 29*, 323.
7. Haseltine, W. A., Block, R., Gilbert, W., and Weber, K. (1972) *Nature 238*, 381.
8. Sy, J., and Lipmann, F. (1973) *Proc. Natl. Acad. Sci. U.S.A. 70*, 306.
9. Hara, A., and Sy, J. (1983) *J. Biol. Chem. 258*, 1678.
10. Heinemeyer, E. A., and Richter, D. (1977) *FEBS Lett. 84*, 357.
11. Avarbock, D., Salem, J., Li, L. S., Wang, Z. M., and Rubin, H. (1999) *Gene 233*, 261.
12. Primm, T. P., Andersen, S. J., Mizrahi, V., Avarbock, D., Rubin, H., and Barry, C. E. (2000) *J. Bacteriol*. (in press).
13. Duggleby, R. (1984) *Comput. Biol. Med. 14*, 455.
14. O'Brien, W. (1976) *Anal. Biochem. 76*, 423.
15. Peterson, E. T., and Uhlenbeck, O. C. (1992) *Biochemistry 31*, 10380.
16. Deobagkar, D. N., and Gopinathan, K. P. (1978) *Can. J. Microbiol. 24*, 693.
17. Ofengand, J., and Chen, C. M. (1972) *J. Biol. Chem. 247*, 2049.
18. Baykov, A. A., Hyytia, T., Volk, S. E., Kasho, V. N., Vener, A. V., Goldman, A., Lahti, R., and Cooperman, B. S. (1996) *Biochemistry 35*, 4655.
19. Kaziro, Y. (1959) *J. Biochem. 46*, 1523.
20. Haseltine, W. A., and Block, R. (1973) *Proc. Natl. Acad. Sci. U.S.A. 70*, 1564.
21. Sassanfar, M., Kranz, J. E., Gallant, P., Schimmel, P., and Shiba, K. (1996) *Biochemistry 35*, 9995.
22. Kim, S., Jo, Y. J., Lee, S. H., Motegi, H., Shiba, K., Sassanfar, M., and Martinis, S. A. (1998) *FEBS Lett. 427*, 259.
23. Levin, J. G. (1970) *J. Biol. Chem. 245*, 3195.
24. Frick, D. N., Weber, D. J., Gillespie, J. R., Bessman, M. J., and Mildvan, A. S. (1994) *J. Biol. Chem. 269*, 1794.
25. Mildvan, A. S., Weber, D. J., and Abeygunawardana, C. (1999) *Adv. Enzymol. Relat. Areas Mol. Biol. 73*, 183.
26. Slater, J. P., Tamir, I., Loeb, L. A., and Mildvan, A. S. (1972) *J. Biol. Chem. 247*, 6784.
27. Dutta, R., and Inouye, M. (1996) *J. Biol. Chem. 271*, 1424.
28. Jaggi, R., van Heeswijk, W. C., Westerhoff, H. V., Ollis, D. L., and Vasudevan, S. G. (1997) *EMBO J. 16*, 5562.
29. Kwon, D. S., Lin, C. H., Chen, S., Coward, J. K., Walsh, C. T., and Bollinger, J. M. (1997) *J. Biol. Chem. 272*, 2429.
30. Yuen, M. H., Wang, X., Mizuguchi, H., Uyeda, K., and Hasemann, C. A. (1999) *Biochemistry 38*, 12333.
31. Miller, S. P., Karschnia, E. J., Ikeda, T. P., and LaPorte, D. C. (1996) *J. Biol. Chem. 271*, 19124.
32. Frolova, L., Goff, X. L., Zhouravleva, G., Davydova, E., Philippe, M., and Kisselev, L. (1996) *RNA 2*, 334.
33. Voigt, J., and Nagel, K. (1993) *J. Biol. Chem. 268*, 100.
34. Piepenburg, O., Pape, T., Pleiss, J. A., Wintermeyer, W., Uhlenbeck, O. C., and Rodnina, M. V. (2000) *Biochemistry 39*, 1734.
35. Cate, J. H., Yusupov, M. M., Yusupova, G. Z., Earnest, T. N., and Noller, H. F. (1999) *Science 285*, 2095.

BI001256K